HHS Public Access

Author manuscript

Immunol Cell Biol. Author manuscript; available in PMC 2017 November 03.

Published in final edited form as:

Immunol Cell Biol. 2017 September ; 95(8): 684–694. doi:10.1038/icb.2017.38.

CD8 T cells contribute to lacrimal gland pathology in the nonobese diabetic mouse model of Sjögren syndrome

Jennifer Y. Barr[1], **Xiaofang Wang**[1], **David K. Meyerholz**[2], and **Scott M. Lieberman**[1,3]

[1]Stead Family Department of Pediatrics, University of Iowa, Iowa City, IA, USA

[2]Department of Pathology, Carver College of Medicine, University of Iowa, Iowa City, IA, USA

[3]Interdisciplinary Graduate Program in Immunology, University of Iowa, Iowa City, IA, USA

Abstract

Sjögren syndrome is an autoimmune disease characterized by targeted destruction of the lacrimal and salivary glands resulting in symptoms of severe ocular and oral dryness. Despite its prevalence, the mechanisms driving autoimmune manifestations are unclear. In patients and in the nonobese diabetic (NOD) mouse model of Sjögren syndrome, lymphocytic infiltrates consist of CD4 and CD8 T cells, although the role of CD8 T cells in disease pathogenesis has been largely unexplored. Here, we evaluated the contribution of CD8 T cells to lacrimal and salivary gland autoimmunity. Within the lacrimal and salivary glands of NOD mice, CD8 T cells were proliferating, expressed an activated phenotype, and produced inflammatory cytokines. Transfer of purified CD8 T cells isolated from the cervical lymph nodes (LN) of NOD mice into NOD-SCID recipients resulted in inflammation of the lacrimal glands, but was not sufficient to cause inflammation of the salivary glands. Lacrimal gland-infiltrating CD8 T cells displayed a cytotoxic phenotype, and epithelial cell damage in the lacrimal glands was observed in recipients of CD8 T cells regardless of the presence of CD4 T cells. Collectively, our results demonstrate that CD8 T cells play a pathogenic role in lacrimal gland autoimmunity. The gland-specific pathogenicity of CD8 T cells makes them a valuable resource to further understand the mechanisms that discriminate lacrimal versus salivary gland autoimmunity and for the development of new therapeutics that target the early stages of disease.

Introduction

Sjögren syndrome is a complex autoimmune disease characterized by targeted immune destruction of the lacrimal and salivary glands. Damage to the glands leads to the loss of appropriate tear and saliva production resulting in symptoms of severe dry eyes and mouth

Corresponding Author: Scott M. Lieberman, Stead Family Department of Pediatrics, Carver College of Medicine, University of Iowa, 500 Newton Road, 2191 Medical Laboratories, Iowa City, IA 52242, USA, Phone: (319) 353-4399, Fax: (319) 356-2341, scott-lieberman@uiowa.edu.

Conflict of Interest

The authors have no competing financial or commercial conflicts of interest to disclose.

The authors declare no conflicts of interest.

Supplementary information is available at *Immunology & Cell Biology*'s website.

that decrease quality of life and cause considerable morbidity[1]. In addition, other organs may be targeted by the aberrant immune response, and patients with Sjögren syndrome have an increased risk of developing lymphoma[2]. Despite the high prevalence of disease, the etiology of Sjögren syndrome is poorly understood, in part due to the difficulty in studying the early cellular events, which arise years prior to clinical symptoms[3].

The nonobese diabetic (NOD) mouse spontaneously develops lacrimal and salivary gland autoimmunity, and is a well-characterized model of Sjögren syndrome[4, 5]. In NOD mice, sex-specific differences in gland inflammation have been described, with male mice developing spontaneous lacrimal gland inflammation (dacryoadenitis) and female mice developing spontaneous salivary gland inflammation (sialadenitis)[6–10]. Lymphocytic infiltrates isolated from the lacrimal and salivary glands of humans and NOD mice are composed largely of CD4 T cells, yet CD8 T cells are consistently present[11–16]. In a variety of other autoimmune diseases, CD8 T cells contribute to the initiation, progression, or regulation of disease and, depending on the context, both pathogenic and regulatory roles have been described[17–30]. However, the role of CD8 T cells in lacrimal or salivary gland autoimmunity is not known.

Here, we evaluate the phenotype of CD8 T cells in lacrimal and salivary gland infiltrates in NOD mice and use a previously described adoptive transfer model[6] to dissect the roles of CD8 T cells in lacrimal and salivary gland autoimmunity.

Results

Activated CD8 T cells are present in lacrimal and salivary gland infiltrates

To determine the role of CD8 T cells in lacrimal and salivary gland autoimmunity, we characterized CD8 T cells isolated from the lacrimal and salivary glands of male and female NOD mice, respectively. As previously demonstrated[12], the frequencies of CD4 and CD8 T cells were similar in infiltrates from lacrimal and salivary glands, with CD4 T cells constituting the majority of T cells in each gland, but with a population of CD8 T cells always present (Figure 1a). We assessed these CD8 T cells in gland infiltrates for the expression of surface activation markers and production of cytokines (Figure 1b). This included analysis of the integrin CD11a, which plays a role in T cell co-stimulation[31, 32] and is upregulated on CD8 T cells after antigen stimulation[33], thus serving as a surrogate marker for T cell activation. We also examined cell surface expression of CD69, which is upregulated as a result of T cell stimulation through the T cell receptor[34], or in the presence of inflammatory signals (e.g., interferon-α/β)[35]. In both lacrimal and salivary glands, the majority of CD8 T cells expressed CD11a, while a large subset also expressed CD69 (Figure 1b). A subset of CD8 T cells isolated from the glands was actively proliferating based on Ki67 staining (Figure 1b). The majority of CD8 T cells produced IFNγ upon stimulation, and a subset of these co-produced TNFα (Figure 1b). Similarly, lacrimal and salivary gland-infiltrating CD4 T cells expressed an activated phenotype, were proliferating, and produced IFNγ and TNFα following stimulation (Figure 1c). Thus, the majority of CD8 and CD4 T cells in lacrimal and salivary gland infiltrates displayed an activated phenotype and were capable of producing inflammatory cytokines.

CD8 T cells promote dacryoadenitis, but not sialadenitis

To determine the pathogenicity of CD8 T cells in the context of lacrimal and salivary gland autoimmunity, we tested their ability to promote the development of dacryoadenitis or sialadenitis. To address this question, we utilized our previously established adoptive transfer model of Sjögren syndrome in which the transfer of cervical lymph node (LN) cells into sex-matched recipients results in gland inflammation similar to that observed in spontaneous disease[6] (and manuscript in preparation). CD8 T cells were purified (>96% of total cells and >98% of T cells) from cervical LN of male or female NOD mice and transferred into sex-matched NOD-SCID recipients (Figure 2a). As a comparison, we transferred purified CD8 T cells that were re-combined with the CD8-depleted population (nonCD8+CD8) into sex-matched NOD-SCID recipient mice. Five weeks after transfer, the degree of dacryoadenitis or sialadenitis was assessed. In male recipients, a similar level of dacryoadenitis developed in mice that received CD8 only cells relative to mice that received nonCD8+CD8 cells, with some mice in the CD8 only group developing diffuse inflammation (Figure 2b and Supplemental Figure 1a). While low levels of sialadenitis were observed in some recipients of nonCD8+CD8 cells, sialadenitis was not observed in male recipients of CD8 only cells (Figure 2b and Supplemental Figure 1b). In the NOD mouse model, male mice spontaneously develop dacryoadenitis, whereas a greater degree of sialadenitis develops in female NOD mice[8, 9]. Therefore, we determined if CD8 T cells could promote sialadenitis in female mice. Strikingly, while female recipients of nonCD8+CD8 cells developed sialadenitis, we did not detect sialadenitis in any female NOD-SCID recipients of CD8 only cells, despite the fact that some of these recipients developed dacryoadenitis (Figure 2c and Supplemental Figures 1c and 1d). Collectively, these data suggest that CD8 T cells can independently promote the development of dacryoadenitis in male NOD mice but not sialadenitis in female NOD mice.

Flow cytometric analyses of cervical LN cells in recipient mice 5 weeks after transfer confirmed that recipients of CD8 only cells had proportionally more CD8 T cells in the cervical LN relative to mice that received nonCD8+CD8 cells (Figure 2d). An outgrowth of CD4 T cells was observed in CD8 only recipients, yet this percentage was still significantly reduced relative to the percentage of CD4 T cells present in recipients of nonCD8+CD8 cells (Figure 2d). The outgrowth of CD4 T cells in the cervical LN of CD8 only recipients included a subset of $CD4^{+}Foxp3^{+}$ Tregs (Supplemental Figure 2a). Corresponding to the overall reduction in the percentage of CD4 T cells in CD8 only recipients, the percentage of Tregs within the total T cell population was also significantly reduced relative to recipients of nonCD8+CD8 cells (Supplemental Figure 2a). However, within the CD4 T cell population the percentage of Tregs was similar in CD8 only recipients relative to recipients of nonCD8+CD8 cells (Supplemental Figure 2b), suggesting that the outgrowth of CD4 T cells in the cervical LN is equivalent for nonTregs and Tregs. Despite the outgrowth of CD4 T cells in recipients of CD8 only cells, very few B cells were present, whereas recipients of nonCD8+CD8 cells had an appreciable proportion of B cells (Supplemental Figure 2c).

Analysis of cell composition in the lacrimal glands similarly showed that CD8 T cells comprised the major cell population in CD8 only recipients, yet the outgrowth of CD4 T cells noted in the cervical LN was also detected within these lacrimal gland infiltrates

(Figure 2e). In recipients of nonCD8+CD8 cells, CD4 T cells constituted the majority of cells in the lacrimal glands, while CD8 T cells comprised a small subset of the population (Figure 2e), similar to the composition observed in spontaneous disease (Figure 1). Notably, the ratio of CD4:CD8 T cells was elevated within the lacrimal glands relative to the cervical LN in mice that received nonCD8+CD8 cells (Figure 2f), indicating a selectivity for CD4 T cells in the lacrimal glands, similar to that observed when dacryoadenitis develops spontaneously (Figure 2g). Although not significant, a similar difference was also observed in recipients of CD8 only cells (Figure 2f). However, whether this reflects differential trafficking of CD4 T cells to the lacrimal glands or differential expansion of these cells within the lacrimal glands remains to be determined. Within the total T cell population in the lacrimal glands, $CD4^+Foxp3^+$ Tregs were also significantly reduced in CD8 only recipients relative to recipients of nonCD8+CD8 cells (Supplemental Figure 2d). While not reaching statistical significance, $CD4^+Foxp3^+$ Tregs were reduced within the $CD4^+$ population in CD8 only recipients relative to recipients of nonCD8+CD8 cells (Supplemental Figure 2e). This is in contrast to the cervical LN (Supplemental Figure 2b), although it is unclear if this is due to differences in the trafficking of $CD4^+Foxp3^+$ cells to the lacrimal glands or their expansion within the glands.

Dacryoadenitis occurs in the absence of CD8 T cells

Despite the presence of activated CD8 T cells in lacrimal gland infiltrates, the outgrowth of CD4 T cells in our CD8 only transfers and selective accumulation of CD4 T cells within lacrimal glands of NOD mice and NOD-SCID recipients suggested CD4 T cells play a key role in the development of dacryoadenitis. To determine if cervical lymph node cells could mediate lacrimal gland disease in the absence of CD8 T cells, we transferred CD8-depleted cervical LN cells from male NOD donors either alone (nonCD8) or with CD8 T cells added back (nonCD8+CD8) to sex-matched, NOD-SCID recipient mice. A similar degree of dacryoadenitis developed in recipients of nonCD8 cells and recipients of nonCD8+CD8 cells (Figure 3a). In contrast to the outgrowth of CD4 T cells observed in CD8 only transfers (Figure 2d–2f), very few (<1%) CD8 T cells were detected in the cervical LN or lacrimal glands of recipients of nonCD8 cells (Figure 3b, 3c). Analysis of other lymphocyte populations demonstrated both CD4 T cells and B cells were present, with no difference in the percentage of B cells observed between the two groups (Figure 3b, 3c and Supplemental Figure 3). Thus, CD8-depleted cervical LN cells can transfer dacryoadenitis.

CD8 and CD4 T cells each contribute to dacryoadenitis

We next assessed the level of spontaneous dacryoadenitis in NOD mice that were deficient for *CD8* expression ($CD8^{null}$) or *CD4* expression ($CD4^{null}$) and thus lacked CD8 or CD4 T cells, respectively. In contrast to our transfer model, the absence of CD8 T cells resulted in a significant decrease in dacryoadenitis in 11–14-week-old $CD8^{null}$ mice relative to age-matched wild-type (WT) NOD mice (Figure 4). Dacryoadenitis was also significantly reduced in $CD4^{null}$ mice relative to WT controls, while no difference in inflammation was observed between $CD8^{null}$ and $CD4^{null}$ mice (Figure 4). In contrast, 20–24-week-old $CD8^{null}$ mice developed increased dacryoadenitis relative to age-matched $CD4^{null}$ mice, which continued to display decreased dacryoadenitis compared to age-matched WT mice (Figure 4). Further, the degree of inflammation in old $CD8^{null}$ mice was increased relative to

young *CD8*^{null} mice, whereas no change was observed between young and old *CD4*^{null} mice (Figure 4). For all genotypes, both T and B cells were present in the cervical LN and, as expected, CD8 or CD4 T cells were absent from the cervical LN of *CD8*^{null} or *CD4*^{null} mice, respectively (Supplemental Figure 4). Collectively, these findings suggest that whereas CD8 T cells do not compensate for the lack of CD4 T cells, over time CD4 T cells can compensate for the lack of CD8 T cells in mediating dacryoadenitis.

Although the degree of dacryoadenitis in 11–14-week-old *CD8*^{null} and *CD4*^{null} mice was reduced relative to WT NOD mice, some inflammation was still observed (i.e., focus score > 0), which is in contrast to mouse strains that are not prone to lacrimal gland autoimmunity. Specifically, no foci (i.e., focus score = 0) were observed in lacrimal glands of 13-week-old male Balb/c mice ($n = 5$, data not shown). These data indicate that CD8 and CD4 T cells are independently capable of mediating some degree of lacrimal gland inflammation in NOD mouse strains. Collectively, the reduction in disease severity in the absence of either CD8 or CD4 T cells suggests that both cell types contribute to the early events that promote spontaneous dacryoadenitis.

CD4 T cells are not required for CD8 T cell-mediated dacryoadenitis

Although the development of some dacryoadenitis in *CD4*^{null} mice suggests inflammation in this context is mediated by CD8 T cells, the presence of $CD4^{-}CD8^{-}TCR\alpha\beta^{+}$ T cells with characteristics of CD4 T cells have been reported in *CD4*^{null} mice[36]. Thus, we cannot rule out the potential contribution of these cells to the dacryoadenitis observed in *CD4*^{null} mice. Additionally, the consistent outgrowth of CD4 T cells in our CD8 only transfers (Figure 2d–2f) suggested the possibility that CD8 T cells only cause dacryoadenitis in the presence of CD4 T cells. To address this, we transferred purified populations of FACS-sorted CD8 T cells from male NOD donors (Figure 5a) into sex-matched, NOD-SCID recipients that were treated weekly with anti-CD4 or isotype control antibody. Similar to the outgrowth of CD4 T cells observed in our prior CD8 only transfers, an outgrowth of CD4 T cells was detected at 3 and 5 weeks post transfer in the peripheral blood of recipient mice treated with an isotype control antibody (Figure 5b). In contrast, CD4 T cells were undetectable in the blood of mice receiving the anti-CD4 antibody treatment (Figure 5b), indicating efficient depletion of CD4 T cells. Despite these differences, the degree of dacryoadenitis was similar in mice treated with anti-CD4 antibody relative to those treated with isotype control antibody (Figure 5c). The overwhelming majority of cells recovered from the cervical LN or lacrimal glands of anti-CD4 antibody treated recipients were CD8 T cells, with <0.6% being CD4 T cells (Figure 5d, 5e). Importantly, while the CD4:CD8 ratio again demonstrated an increase in CD4 T cells in the lacrimal glands relative to the cervical LN of isotype antibody treated recipients, no such accumulation was noted in the lacrimal glands of anti-CD4 antibody treated recipients (Figure 5f). Thus in the absence of an outgrowth of CD4 T cells, CD8 T cells can independently infiltrate the lacrimal glands and promote the development of dacryoadenitis in our transfer model of Sjögren syndrome.

CD8 T cells mediate epithelial cell destruction

The presence of activated, inflammatory cytokine-producing CD8 T cells in the lacrimal glands (Figure 1) and the ability of CD8 T cells to promote the development of

dacryoadenitis even in the absence of CD4 T cells (Figure 5) suggest CD8 T cells play a pathogenic role in lacrimal gland autoimmunity. Upon activation, CD8 T cells differentiate into cytotoxic T cells and kill target cells when their cognate antigen is recognized[29]. To confirm that CD8 T cells in the lacrimal glands mediate epithelial cell damage, we assessed epithelial cell apoptosis by staining for activated caspase-3 in lacrimal gland sections from prior recipients of nonCD8+CD8 or CD8 only cells, or from male NOD mice that developed spontaneous dacryoadenitis. Selected recipients with focus scores similar to the median focus score of their respective group were chosen for analysis: nonCD8+CD8 (median focus score: 2.8; range: 2.2–3.2), CD8 only T cells (median focus score: 3.5; range: 1.6–9.2), male NOD mice with spontaneous dacryoadenitis (median focus score: 8.3; range: 5.0–15.4). Additionally, recipients with no focal inflammation (i.e., focus score = 0) from each of these transfer groups were analyzed to establish baseline levels of activated caspase-3 expression. In the absence of inflammation infrequent activated caspase-3 staining was observed (0.7 activated caspase-3^+ cells/mm^2 +/− 0.5; $n = 3$). The total number of activated caspase-3^+ cells was increased over baseline levels in nonCD8+CD8 recipient mice with inflammation (2.0 activated caspase-3^+ cells/mm^2 +/− 2.4; $n = 7$), in CD8 only recipients with inflammation (4.1 activated caspase-3^+ cells/mm^2 +/− 2.3; $n = 7$), and in mice with spontaneous inflammation (3.7 activated caspase-3^+ cells/mm^2 +/− 1.1; $n = 6$), although these differences did not reach statistical significance (one-way ANOVA $P = 0.059$). Therefore, to determine if the activated caspase-3 staining observed in the presence of inflammation could be distinguished from that observed in areas not associated with inflammation, we assessed the number of activated caspase-3^+ cells based on location: within inflammatory foci (in), outside of inflammatory foci (out) (Figure 6a), or in areas of normal tissue (normal) (Figure 6b). Within each group, more activated caspase-3^+ cells were within inflammatory foci than those in the adjacent region outside of the inflammation or in areas of normal tissue (Figure 6c). These data suggested an association of epithelial cell apoptosis with inflammatory foci, which makes biological sense. However, to mitigate potential bias associated with analysis of select areas within tissue sections, we quantified the number of activated caspase-3^+ cells from whole tissue sections of glands from recipients of CD8 only cells, recipients of nonCD8+CD8 cells, and male NOD mice with spontaneous disease. To confirm our findings above, we compared the total number of activated caspase-3^+ cells (normalized to tissue section area) to the total number of foci (normalized to area) quantified from separate H&E-stained tissue sections for each sample. As expected, these whole-slide analyses demonstrated correlation between cell death and inflammation (Figure 6d). Taken together, these findings demonstrate epithelial cell death is associated with lacrimal gland inflammation and suggest that CD8 T cells are capable of mediating lacrimal gland epithelial cell death.

As mice in the CD8 only group included some recipients with CD4 T cell outgrowth and also those treated with depleting antibody to prevent such outgrowth, we wanted to confirm that the number of activated caspase-3^+ cells in CD8 only recipients was not dependent on an outgrowth of CD4 T cells. Thus, we assessed the correlation between the number of activated caspase-3^+ cells within areas of inflammation and the percentage of CD4 T cells in the lacrimal gland five weeks after transfer. No correlation was observed between the number of activated caspase-3^+ cells detected in inflammatory foci and the percentage of

CD4 T cells within the gland (Figure 6e). Thus, these data demonstrate that epithelial cell apoptosis observed in mice with dacryoadenitis is associated with the inflammatory infiltrate in the lacrimal glands and is similar whether CD8 T cells are alone or are accompanied by other cells (e.g., CD4 T cells).

One mechanism of cell killing utilized by CD8 T cells is through the release of cytotoxic granules containing perforin and granzyme B[37, 38]. Release of these molecules is the result of degranulation, which occurs rapidly after cell activation[38]. As a consequence of degranulation, CD8 T cells express the lysosomal associated membrane glycoprotein CD107a on their surface, and this correlates with cytotoxic activity[39]. Thus, measuring surface expression of CD107a identifies CD8 T cells that have undergone degranulation. To determine if CD8 T cells in the lacrimal glands displayed characteristics of cytotoxic CD8 T cells, we used flow cytometric analyses to assess the expression of CD107a and granzyme B. Assessment of lacrimal gland infiltrates isolated from male NOD mice that developed spontaneous dacryoadenitis demonstrated an increased proportion of CD8 T cells that expressed CD107a after stimulation *ex vivo* relative to CD8 T cells in the cervical LN (Figure 6f). Additionally, a smaller but significant increase in the percentage of CD8 T cells producing granzyme B was observed in lacrimal gland infiltrates relative to those from the cervical LN (Figure 6f). Thus, a subset of CD8 T cells within the lacrimal glands displayed a cytotoxic phenotype. Collectively, these data indicate that CD8 T cells contribute to spontaneous dacryoadenitis and induce apoptosis of lacrimal gland epithelial cells, suggesting a pathogenic role for CD8 T cells in autoimmune dacryoadenitis.

Discussion

CD8 T cells contribute to disease pathogenesis in a variety of autoimmune diseases[17–20, 28–30]. For example, CD8 T cells are required for the initiation of autoimmune diabetes[18, 19] and are the primary pathogenic effector cells in primary biliary cirrhosis[17]. However, it is also well established that CD8 T cells can play a regulatory role in the context of autoimmunity[21]. In humans with autoimmune diabetes or relapsing-remitting multiple sclerosis, a decrease in the $CD8^{+}CD28^{-}$ suppressor T cell population has been observed[22]. Additionally, regulatory CD8 T cells have been described in animal models of autoimmune diabetes[25] and in experimental autoimmune encephalomyelitis (EAE)[23, 24, 27], the animal model for multiple sclerosis. Thus, evidence exists for both pathogenic and regulatory roles for CD8 T cells in the context of autoimmunity.

In Sjögren syndrome, CD8 and CD4 T cells are present in lacrimal and salivary gland infiltrates from both humans and NOD mice[11–16]. CD4 T cells constitute the major T cell present in gland infiltrates, and numerous studies have investigated the contributions from these cells in Sjögren syndrome[40]. Yet despite the consistent presence of CD8 T cells in the lacrimal and salivary glands, it is unclear how these cells contribute to the development or progression of lacrimal gland autoimmunity. Analysis of human lacrimal gland infiltrates from patients with Sjögren syndrome found CD8 T cells clustered around apoptotic acinar epithelial cells, and increased expression of effector molecules was observed, suggesting the cell death was mediated by CD8 T cells[11]. A recent study found increased activated CD8 T cells in the circulation of Sjögren syndrome patients with higher disease activity[16]. In

contrast, a role for regulatory CD8 T cells has been described in a desiccating stress model resembling Sjögren syndrome[41]. However, the role of CD8 T cells in the NOD mouse model of Sjögren syndrome has not been previously explored.

Our study demonstrates that within the lacrimal glands of male NOD mice, CD8 T cells displayed an activated phenotype, produced inflammatory cytokines upon stimulation, and expressed markers indicative of cytotoxicity. Using an adoptive transfer model, our study provides evidence that CD8 T cells can independently promote dacryoadenitis and mediate epithelial cell damage. Thus, our data suggest CD8 T cells play a pathogenic role in lacrimal gland autoimmunity.

The majority of CD8 T cells isolated from the lacrimal and salivary glands of NOD mice produced IFNγ following *ex vivo* stimulation, suggesting a potential mechanism by which they contribute to disease. IFNγ has multiple biological effects, including immune-cell activation, induction of chemokines and adhesion molecules on immune and nonimmune cells, and promotion of apoptosis[42]. A pathogenic role for IFNγ has been observed in autoimmune diseases such as autoimmune diabetes[43, 44], systemic lupus erythematosus[45, 46], and rheumatoid arthritis[42, 47], and elevated levels of IFNγ were reported in Sjögren syndrome patients[48, 49]. In NOD mice, IFNγ was required for the development of salivary gland autoimmunity[50]. IFNγ was shown to alter tight junction integrity and function in parotid gland epithelial cells[51] and to induce salivary gland cell death[52]. Further, the chemokines CXCL9 and CXCL10, which were increased in salivary gland lesions from patients with Sjögren syndrome, were induced by IFNγ in primary salivary gland epithelial cells[53]. Thus, IFNγ likely plays a pathogenic role in salivary gland disease through multiple mechanisms. Levels of CXCL9 and CXCL10 were also increased in tears from Sjögren syndrome patients[54] suggesting IFNγ may play a similar role in lacrimal gland pathology. Our findings demonstrating that CD8 T cells produce IFNγ and mediate epithelial cell death in NOD mouse lacrimal glands. Thus, IFNγ likely contributes to lacrimal gland pathology through multiple mechanisms.

Because the NOD mouse model displays sex-specific differences in gland inflammation, with dacryoadenitis occurring in male mice and sialadenitis occurring in female mice[6–10], we independently studied male and female mice for the development of lacrimal and salivary gland disease, respectively. As in the male lacrimal glands, CD8 T cells were present in salivary gland infiltrates from female NOD mice, showed signs of activation, and produced inflammatory cytokines. These cytokine-producing T cells were relatively more abundant within lacrimal glands, which may reflect differences in the mechanisms of disease development; however, this could also be explained by differences in the kinetics of lacrimal or salivary gland disease development. More strikingly apparent was the finding that CD8 T cells caused dacryoadenitis when transferred into male recipients but were completely incapable of mediating sialadenitis in female recipients. While no difference in lacrimal gland inflammation was noted on a population level between female recipients of purified CD8 T cells and nonCD8+CD8 T cells, we were surprised to find that some female recipients of purified CD8 T cells developed dacryoadenitis with focus scores greater than the median focus scores of male recipients. This is in contrast to NOD female mice or NOD-SCID female recipients of nonCD8+CD8 cells, which develop little or no lacrimal gland

autoimmunity. Previously, we have shown that female NOD mice are protected from developing dacryoadenitis due to the presence of lacrimal gland-protective Tregs[6]. One possibility here is that the transfer of purified CD8 T cells, which were largely devoid of Tregs, resulted in dacryoadenitis simply due to the lack of lacrimal gland-protective Tregs. However, the complete absence of sialadenitis in those same recipients makes this explanation less likely because, in our hands, adoptive transfer of Treg-depleted cells (inclusive of both CD4 and CD8 T cells) results in both dacryoadenitis and sialadenitis in recipients regardless of sex (manuscript in preparation). Thus, our studies demonstrate a unique role for CD8 T cells in mediating lacrimal gland-specific inflammation in the absence of CD4 T cells.

Our studies expand previous findings that distinct mechanisms drive lacrimal and salivary gland autoimmunity. Differences in gland infiltration have been observed in NOD mice that are deficient for *IFNγ* or *IFNγR* expression[50]. In this context, focal infiltrates in the salivary glands of NOD.$IFN\gamma^{-/-}$ or NOD.$IFN\gamma R^{-/-}$ mice were absent at 20 weeks of age, similar to the salivary glands from non-autoimmune, age-matched C57BL/6 mice, and in contrast to the parental NOD strain. However, leukocyte infiltrates were still observed in the lacrimal glands of NOD.$IFN\gamma^{-/-}$ or NOD.$IFN\gamma R^{-/-}$ mice at levels similar to that observed in NOD mice[50]. Additionally, distinct susceptibility loci were linked to the development of dacryoadenitis and sialadenitis in the MRL/lpr mouse model of Sjögren syndrome[55]. Thus, evidence from our study and others suggests that inflammation of the lacrimal and salivary glands can arise through distinct mechanisms.

In our adoptive transfer studies, we observed variability in disease development with some recipients failing to develop lacrimal gland inflammation. This is similar to the variability we have previously observed in this adoptive transfer model[6] and likely reflects multiple factors. We developed this adoptive transfer model to study the early immunological events in lacrimal and salivary gland autoimmunity and believe the lack of all recipients being affected by 5 – 7 weeks post-transfer is indicative of such an early stage in disease development. Sjögren syndrome-like disease in NOD mice is an immunologically complex disease as reflected by the variability in degree of lacrimal gland inflammation even in the spontaneous disease[6]. In that study, spontaneous disease in 6 – 12 week old male NOD mice demonstrated variable focus scores; however, all mice in that analysis had developed some degree of dacryoadenitis and, in general, the focus scores in spontaneous disease were greater than those in the adoptive transfer model. It is unclear whether these differences in the transfer and spontaneous models suggest that the transfer model represents a very early stage in disease development or, rather, that other factors contributing to spontaneous disease development are not optimized in the transfer model. Regardless, it is striking that despite the variability in disease development in our adoptive transfer model, our data clearly demonstrate a pathogenic role for CD8 T cells in lacrimal gland autoimmunity including a role in mediating lacrimal gland epithelial cell death. Beyond the lacrimal glands, the ocular surface is another key site of inflammatory damage in Sjögren syndrome. Whether the pathogenic role for CD8 T cells extends similarly to the ocular surface in NOD mice was not evaluated in our studies. Interestingly, studies in a desiccating stress model demonstrated a regulatory role for CD8 T cells at the ocular surface, so further studies into the role of CD8 T cells in ocular surface inflammation in NOD mice are warranted.

In addition to a pathogenic role for CD8 T cells, our studies here also further support the key role of CD4 T cells in lacrimal gland autoimmunity as evidenced by the outgrowth of CD4 T cells and their enrichment within lacrimal glands in our CD8 only transfer studies. Because we focused on CD8 T cells in these studies, we did not evaluate for phenotypic differences in the outgrowing CD4 T cell population compared to CD4 T cells in nonCD8+CD8 transfers, nonCD8 transfers, or spontaneous disease. Further study of these CD4 T cell populations may provide insight into the specific mechanisms of pathogenic CD4 T cell involvement in lacrimal gland autoimmunity. Regardless, our data demonstrate that even when the outgrowth of CD4 T cells is prevented, CD8 T cells are capable of mediating lacrimal gland autoimmunity.

Understanding the initiation of a complex autoimmune disease such as Sjögren syndrome requires knowledge of all of the cellular players involved in the immune response. Our work here describes a pathogenic role for CD8 T cells in the early stages of dacryoadenitis. Further insight into the mechanisms that are required for CD8 T cells to overcome immune tolerance will help in understanding the events that lead to the development of organ specific autoimmunity.

Methods

Mice

Male and female NOD/ShiLtJ (NOD), NOD.CB17-*Prkdc*^{scid}/*J* (NOD-SCID), NOD.129S6(B6)-*CD4*^{tm1knw}/DvsJ (*CD4*^{null}), and Balb/cJ mice were purchased from The Jackson Laboratory (Bar Harbor, ME). Male and female NOD.129S2(B6)-*CD8a*^{tm1Mak}/DvsJ (*CD8*^{null}) mice were kindly provided by David Serreze (The Jackson Laboratory). NOD mice expressing the bicistronic Foxp3-green fluorescent protein (GFP) (NOD), obtained by backcrossing the Foxp3-GFP knock-in C57BL/6J mice[56] for > 20 generations onto the NOD background, were a kind gift from Vijay Kuchroo (Harvard University). For transfer studies, donor mice were 5–6 weeks old and recipients were 7–9 weeks old. For *ex vivo* analyses, mice were 12–17 weeks old. The exact sample size (*n*) and biological and experimental replicates are indicated in each figure legend. Samples sizes were determined based on previous transfer studies and typically included 10–15 mice per group pooled from multiple experiments. All mice were monitored for the presence of glucosuria using Diastix urine dipsticks (Bayer Diagnostics, Whippany, NJ). A positive test was indicative of autoimmune diabetes development. Mice were maintained and used in accordance with the University of Iowa Institutional Animal Care and Use Committee Guidelines.

Histological characterization of inflammation in lacrimal and salivary glands

Exorbital lacrimal and submandibular salivary glands were harvested and fixed in buffered formalin, processed, embedded in paraffin, and sectioned. Five micrometer sections of paired glands were stained with hematoxylin and eosin (H&E) and analyzed by standard light microscopy. Inflammation was quantified using standard focus scoring[57]. Focus scores (number of inflammatory foci per 4 mm^2) were calculated by a blinded observer by counting the total number of foci (composed of ≥ 50 mononuclear cells) by standard light microscopy using a 10× objective, scanning slides to obtain digital images using PathScan Enabler IV

(Meyer Instruments), and measuring surface area of sections using ImageJ software[58]. Samples with diffuse inflammation resulting in coalescence of individual foci were assigned focus score values greater than the highest calculable value for that set of comparisons. Representative images were captured on a Leitz DM-RB research microscope with a Leica DCF700T digital camera using Leica Application Suite X software (Leica Microsystems, Wetzlar, Germany).

Lymphocyte isolation

Cervical LN or spleens were dissociated with the end of a 3 mL syringe plunger through 70 μM nylon mesh in RPMI (Life Technologies, Waltham, MA) supplemented with 10% FBS, 100 U/mL penicillin, 100 μg/mL streptomycin, and 50 μM β-mercaptoethanol (complete RPMI). Cells were treated with ACK lysis buffer (Lonza, Mapleton, IL) to remove red blood cells (RBC). To isolate cells from the lacrimal or salivary glands, glands were incubated in Collagenase type IV (Life Technologies, Waltham, MA) at 37°C with shaking for 1 or 1.5 hours, respectively. Glands were then dissociated with the end of a 3 mL syringe plunger through 40 μM nylon mesh and RBC lysed as above to obtain single cell suspensions. Peripheral blood samples were collected through the retro-orbital plexus and diluted in PBS containing 20 U/mL heparin sodium (Fisher Scientific, Hampton, NH). Single cell suspensions were obtained using Histopaque-1083 (Sigma-Aldrich, St. Louis, MO) according to the manufacturer's instructions.

Flow cytometry and FACS

Cells from cervical LN, lacrimal or salivary glands, or peripheral blood were analyzed by flow cytometry using a BD LSR II or BD Acurri C6 (BD Biosciences, San Jose, CA) for acquisition and FlowJo software (Treestar, Inc., Ashland, OR) for analysis. All samples were gated initially on forward and side scatter parameters to establish the lymphocyte gate then on forward scatter-area by forward scatter-width to establish singlet gates. Specific additional gating noted in figure legends. For live/dead discrimination, cells were stained with a fixable viability dye from eBioscience (San Diego, CA). Intracellular staining was performed using the Foxp3/transcription factor staining buffer set according to the manufacturer's instructions (eBioscience). For CD8-based FACSorting, cells were labeled with a fluorophore-conjugated anti-CD8α monoclonal antibody and sorted into $CD8^+$ and $CD8^-$ populations using a FACS Aria. For analyses of peripheral blood cells from mice treated with anti-CD4 antibody (GK1.5), staining was performed using a different anti-CD4 antibody clone (RM4-5). For cytokine analyses, cells were stimulated for 4 hours at 37°C with Leukocyte Activation Cocktail (with BD GolgiPlug) plus monensin (BD Biosciences) in complete RPMI followed by surface and intracellular staining. For CD107a analysis, cells were stimulated as for cytokine analysis, with the anti-CD107a antibody included during cell stimulation[59]. Antibodies were purchased from BD Biosciences, Biolegend (San Diego, CA), or eBioscience. Antibody clones used were as follows: CD3ε (145-2c11), CD4 (GK1.5 or RM4-5), CD8α (53-6.7), CD11a (2D7), CD69 (H1.2F3), CD107a (1D4B), IFNγ (XMG1.2), Foxp3 (FJK-16s), Ki67 (SolA15), and TNFα (MP6 XT22). Anti-human Granzyme B (GB12) was obtained from Life Technologies.

Transfer model of Sjögren syndrome

Donor cells were isolated from cervical LNs (mandibular, accessory mandibular, and superficial parotid)[60], pooled from several sex-matched NOD mice and adoptively transferred intravenously to sex-matched NOD-SCID recipients. Recipients of different donor cell groups were randomly assigned with each cage housing recipients from multiple groups to avoid a cage effect. Transferred cells included: $1.5–2\times10^6$ purified CD8 T cells (CD8 only), 5×10^6 CD8-depleted cells (nonCD8), or a combination of $1.5–2\times10^6$ CD8 only and 5×10^6 nonCD8 (nonCD8+CD8). 5–7 weeks later organs were harvested for histology and/or flow cytometric analysis. For anti-CD4 treatment, mice received weekly intraperitoneal injections of 100 μg of anti-CD4 antibody (GK1.5) or isotype control antibody (rat IgG2b anti-KLH) (BioXcell, Lebanon, NH) beginning at the time donor cells were transferred. All donors and recipients tested negative for glucosuria at time of euthanasia for tissue harvesting.

Activated caspase-3 staining

Activated caspase-3 immunostaining, which is a recommended and validated technique for detecting and quantifying apoptotic cells in tissue sections[61–66], was performed similar to previous methods[66]. Briefly, paraffin embedded tissues were sectioned (~4μm) onto slides, and hydrated through a series of xylene and alcohol baths. Epitope unmasking was performed using heat-induced antigen retrieval (citrate buffer pH 6.0, 125°C × 25 minutes). Primary antibody was a rabbit polyclonal antibody (1:100, Cat #9661, Cell Signaling Technologies, Danvers, MA). 3,3′-Diaminobenzidine (DAB) was the chromogen, and hematoxylin was the counterstain. Activated caspase-3 staining was quantified using a post-examination masking technique to mitigate bias[67]. Briefly, high resolution images at 200× magnification were collected using a BX51 microscope, DP53 camera, and CellSens software (Olympus Corporation, Center Valley, PA). A defined total area of 0.92 mm^2 was analyzed for each image. Only images in which the entire focus could be observed within the specified area were used for analyses. In a minority of cases, foci were too large to fit in the specified field of view, and these images were excluded from the analysis. Analysis of each image included counting the number of cells staining positive for activated caspase-3 staining and noting the location of each positive cell as either within the inflammatory cell focus (in), outside the inflammatory cell focus but within the specified field of view (out), or in a control image that did not include and was not contiguous to inflammatory cell foci (normal). For each gland, the average number of activated caspase-3^+ cells was obtained from 2 images. For whole-section activated caspase-3^+ cell quantitation, the number of activated caspase-3^+ cells within whole tissue sections from paired glands was obtained. For each sample, the number of activated caspase-3^+ cells was enumerated and normalized to total tissue section area to obtain the number of activated caspase-3^+ cells/mm^2. These data were then used in correlation analyses to determine degree of correlation to the number of foci per mm^2 obtained from H&E-stained sections from the same tissue samples. All analyses were done in a masked fashion.

Statistical analysis

Statistical analyses were performed with Prism software version 6.0 (GraphPad, San Diego, CA) or R version 3.3.2 (R Foundation for Statistical Computing, Vienna, Austria). Mann-Whitney *U*-test was used for two-group comparisons of non-normally distributed data (focus scores). Unpaired Student's t-test was used for two-group comparisons of data that approximated normal distribution (flow cytometry data). Welch's correction was applied to comparisons with significant differences in variance. All two group comparisons were two-tailed. Two-way ANOVA was used for two-dimensional analyses. For two-dimensional analyses of non-normally distributed data, the observed data values were converted to ranks, two-way ANOVA was performed on those ranks, and Tukey's HSD post-hoc test was used to control the alpha level for multiple comparisons. Visual inspection of the residuals yielded no evidence of any model assumptions being violated. Pearson's correlation coefficient was calculated for correlation analysis of normally distributed data. Spearman's correlation coefficient was calculated for correlation analysis of non-normally distributed data. *P* values less than 0.05 were considered significant.

Supplementary Material

Refer to Web version on PubMed Central for supplementary material.

Acknowledgments

The authors gratefully acknowledge Dr. Stanley Perlman for critical reading of the manuscript and helpful suggestions, the Karandikar lab for insightful discussions, Dr. David Serreze and Harold Chapman for assistance with initial $CD8^{null}$ mouse studies, Dr. Vijay Kuchroo for mice, and Dr. Jacob Oleson and Uchechukwu Nwoke for assistance with statistical analyses. This work was supported by the National Institutes of Health (K08 EY022344 to SML) and start-up funds from the Stead Family Department of Pediatrics (SML). The data presented herein were obtained at the Flow Cytometry Facility, which is a Carver College of Medicine / Holden Comprehensive Cancer Center core research facility at the University of Iowa. The Facility is funded through user fees and the generous financial support of the Carver College of Medicine, Holden Comprehensive Cancer Center, and Iowa City Veteran's Administration Medical Center. Research reported in this publication was supported by the National Center for Research Resources of the National Institutes of Health under Award Number 1 S10 OD016199-01A1.

Support for this work provided by the National Institutes of Health (K08 EY022344) to SML and 1 S10 OD016199-01A1 to the University of Iowa Flow Cytometry Facility.

References

1. Mavragani CP, Moutsopoulos HM. Sjogren's syndrome. Annu Rev Pathol. 2014; 9:273–285. [PubMed: 24050623]
2. Maslinska M, Przygodzka M, Kwiatkowska B, Sikorska-Siudek K. Sjogren's syndrome: still not fully understood disease. Rheumatol Int. 2015; 35:233–241. [PubMed: 24985362]
3. Theander E, Jonsson R, Sjostrom B, Brokstad K, Olsson P, Henriksson G. Prediction of Sjogren's Syndrome Years Before Diagnosis and Identification of Patients With Early Onset and Severe Disease Course by Autoantibody Profiling. Arthritis Rheumatol. 2015; 67:2427–2436. [PubMed: 26109563]
4. Delaleu N, Nguyen CQ, Peck AB, Jonsson R. Sjogren's syndrome: studying the disease in mice. Arthritis Res Ther. 2011; 13:217. [PubMed: 21672284]
5. Lee BH, Gauna AE, Pauley KM, Park YJ, Cha S. Animal models in autoimmune diseases: lessons learned from mouse models for Sjogren's syndrome. Clin Rev Allergy Immunol. 2012; 42:35–44. [PubMed: 22105703]

6. Lieberman SM, Kreiger PA, Koretzky GA. Reversible lacrimal gland-protective regulatory T-cell dysfunction underlies male-specific autoimmune dacryoadenitis in the non-obese diabetic mouse model of Sjogren syndrome. Immunology. 2015; 145:232–241. [PubMed: 25581706]
7. Mikulowska-Mennis A, Xu B, Berberian JM, Michie SA. Lymphocyte migration to inflamed lacrimal glands is mediated by vascular cell adhesion molecule-1/alpha(4)beta(1) integrin, peripheral node addressin/l-selectin, and lymphocyte function-associated antigen-1 adhesion pathways. Am J Pathol. 2001; 159:671–681. [PubMed: 11485925]
8. Toda I, Sullivan BD, Rocha EM, Da Silveira LA, Wickham LA, Sullivan DA. Impact of gender on exocrine gland inflammation in mouse models of Sjogren's syndrome. Exp Eye Res. 1999; 69:355–366. [PubMed: 10504269]
9. Hunger RE, Carnaud C, Vogt I, Mueller C. Male gonadal environment paradoxically promotes dacryoadenitis in nonobese diabetic mice. J Clin Invest. 1998; 101:1300–1309. [PubMed: 9502771]
10. Takahashi M, Ishimaru N, Yanagi K, Haneji N, Saito I, Hayashi Y. High incidence of autoimmune dacryoadenitis in male non-obese diabetic (NOD) mice depending on sex steroid. Clin Exp Immunol. 1997; 109:555–561. [PubMed: 9328136]
11. Fujihara T, Fujita H, Tsubota K, Saito K, Tsuzaka K, Abe T, et al. Preferential localization of CD8+ alpha E beta 7+ T cells around acinar epithelial cells with apoptosis in patients with Sjogren's syndrome. J Immunol. 1999; 163:2226–2235. [PubMed: 10438965]
12. Robinson CP, Cornelius J, Bounous DE, Yamamoto H, Humphreys-Beher MG, Peck AB. Characterization of the changing lymphocyte populations and cytokine expression in the exocrine tissues of autoimmune NOD mice. Autoimmunity. 1998; 27:29–44. [PubMed: 9482205]
13. Matsumoto I, Tsubota K, Satake Y, Kita Y, Matsumura R, Murata H, et al. Common T cell receptor clonotype in lacrimal glands and labial salivary glands from patients with Sjogren's syndrome. J Clin Invest. 1996; 97:1969–1977. [PubMed: 8621782]
14. Christodoulou MI, Kapsogeorgou EK, Moutsopoulos HM. Characteristics of the minor salivary gland infiltrates in Sjogren's syndrome. J Autoimmun. 2010; 34:400–407. [PubMed: 19889514]
15. Sakai A, Sugawara Y, Kuroishi T, Sasano T, Sugawara S. Identification of IL-18 and Th17 cells in salivary glands of patients with Sjogren's syndrome, and amplification of IL-17-mediated secretion of inflammatory cytokines from salivary gland cells by IL-18. J Immunol. 2008; 181:2898–2906. [PubMed: 18684981]
16. Mingueneau M, Boudaoud S, Haskett S, Reynolds TL, Nocturne G, Norton E, et al. Cytometry by time-of-flight immunophenotyping identifies a blood Sjogren's signature correlating with disease activity and glandular inflammation. J Allergy Clin Immunol. 2016; 137:1809–1821. e1812. [PubMed: 27045581]
17. Yang GX, Wu Y, Tsukamoto H, Leung PS, Lian ZX, Rainbow DB, et al. CD8 T cells mediate direct biliary ductule damage in nonobese diabetic autoimmune biliary disease. J Immunol. 2011; 186:1259–1267. [PubMed: 21169553]
18. Christianson SW, Shultz LD, Leiter EH. Adoptive transfer of diabetes into immunodeficient NOD-scid/scid mice. Relative contributions of CD4+ and CD8+ T-cells from diabetic versus prediabetic NOD. NON-Thy-1a donors. Diabetes. 1993; 42:44–55. [PubMed: 8093606]
19. DiLorenzo TP, Graser RT, Ono T, Christianson GJ, Chapman HD, Roopenian DC, et al. Major histocompatibility complex class I-restricted T cells are required for all but the end stages of diabetes development in nonobese diabetic mice and use a prevalent T cell receptor alpha chain gene rearrangement. Proc Natl Acad Sci U S A. 1998; 95:12538–12543. [PubMed: 9770521]
20. Hayward SL, Bautista-Lopez N, Suzuki K, Atrazhev A, Dickie P, Elliott JF. CD4 T cells play major effector role and CD8 T cells initiating role in spontaneous autoimmune myocarditis of HLA-DQ8 transgenic IAb knockout nonobese diabetic mice. J Immunol. 2006; 176:7715–7725. [PubMed: 16751419]
21. Tsai S, Clemente-Casares X, Santamaria P. CD8(+) Tregs in autoimmunity: learning "self"-control from experience. Cell Mol Life Sci. 2011; 68:3781–3795. [PubMed: 21671120]
22. Mikulkova Z, Praksova P, Stourac P, Bednarik J, Strajtova L, Pacasova R, et al. Numerical defects in CD8+CD28− T-suppressor lymphocyte population in patients with type 1 diabetes mellitus and multiple sclerosis. Cell Immunol. 2010; 262:75–79. [PubMed: 20219185]

23. Najafian N, Chitnis T, Salama AD, Zhu B, Benou C, Yuan X, et al. Regulatory functions of CD8+CD28− T cells in an autoimmune disease model. J Clin Invest. 2003; 112:1037–1048. [PubMed: 14523041]
24. Abdul-Majid KB, Wefer J, Stadelmann C, Stefferl A, Lassmann H, Olsson T, et al. Comparing the pathogenesis of experimental autoimmune encephalomyelitis in CD4−/− and CD8−/− DBA/1 mice defines qualitative roles of different T cell subsets. J Neuroimmunol. 2003; 141:10–19. [PubMed: 12965249]
25. Tsai S, Shameli A, Yamanouchi J, Clemente-Casares X, Wang J, Serra P, et al. Reversal of autoimmunity by boosting memory-like autoregulatory T cells. Immunity. 2010; 32:568–580. [PubMed: 20381385]
26. Taneja V, Taneja N, Paisansinsup T, Behrens M, Griffiths M, Luthra H, et al. CD4 and CD8 T cells in susceptibility/protection to collagen-induced arthritis in HLA-DQ8-transgenic mice: implications for rheumatoid arthritis. J Immunol. 2002; 168:5867–5875. [PubMed: 12023391]
27. York NR, Mendoza JP, Ortega SB, Benagh A, Tyler AF, Firan M, et al. Immune regulatory CNS-reactive CD8+T cells in experimental autoimmune encephalomyelitis. J Autoimmun. 2010; 35:33–44. [PubMed: 20172692]
28. Walter U, Santamaria P. CD8+ T cells in autoimmunity. Curr Opin Immunol. 2005; 17:624–631. [PubMed: 16226438]
29. Gravano DM, Hoyer KK. Promotion and prevention of autoimmune disease by CD8+ T cells. J Autoimmun. 2013; 45:68–79. [PubMed: 23871638]
30. Petrelli A, van Wijk F. CD8+ T cells in human autoimmune arthritis: the unusual suspects. Nat Rev Rheumatol. 2016; 12:421–428. [PubMed: 27256711]
31. Van Seventer GA, Shimizu Y, Horgan KJ, Shaw S. The LFA-1 ligand ICAM-1 provides an important costimulatory signal for T cell receptor-mediated activation of resting T cells. J Immunol. 1990; 144:4579–4586. [PubMed: 1972160]
32. Bachmann MF, McKall-Faienza K, Schmits R, Bouchard D, Beach J, Speiser DE, et al. Distinct roles for LFA-1 and CD28 during activation of naive T cells: adhesion versus costimulation. Immunity. 1997; 7:549–557. [PubMed: 9354475]
33. Rai D, Pham NL, Harty JT, Badovinac VP. Tracking the total CD8 T cell response to infection reveals substantial discordance in magnitude and kinetics between inbred and outbred hosts. J Immunol. 2009; 183:7672–7681. [PubMed: 19933864]
34. Testi R, D'Ambrosio D, De Maria R, Santoni A. The CD69 receptor: a multipurpose cell-surface trigger for hematopoietic cells. Immunol Today. 1994; 15:479–483. [PubMed: 7945773]
35. Shiow LR, Rosen DB, Brdickova N, Xu Y, An J, Lanier LL, et al. CD69 acts downstream of interferon-alpha/beta to inhibit S1P1 and lymphocyte egress from lymphoid organs. Nature. 2006; 440:540–544. [PubMed: 16525420]
36. Locksley RM, Reiner SL, Hatam F, Littman DR, Killeen N. Helper T cells without CD4: control of leishmaniasis in CD4-deficient mice. Science. 1993; 261:1448–1451. [PubMed: 8367726]
37. Trapani JA, Smyth MJ. Functional significance of the perforin/granzyme cell death pathway. Nat Rev Immunol. 2002; 2:735–747. [PubMed: 12360212]
38. Barry M, Bleackley RC. Cytotoxic T lymphocytes: all roads lead to death. Nat Rev Immunol. 2002; 2:401–409. [PubMed: 12093006]
39. Betts MR, Brenchley JM, Price DA, De Rosa SC, Douek DC, Roederer M, et al. Sensitive and viable identification of antigen-specific CD8+ T cells by a flow cytometric assay for degranulation. J Immunol Methods. 2003; 281:65–78. [PubMed: 14580882]
40. Singh N, Cohen PL. The T cell in Sjogren's syndrome: force majeure, not spectateur. J Autoimmun. 2012; 39:229–233. [PubMed: 22709856]
41. Zhang X, Schaumburg CS, Coursey TG, Siemasko KF, Volpe EA, Gandhi NB, et al. CD8(+) cells regulate the T helper-17 response in an experimental murine model of Sjogren syndrome. Mucosal Immunol. 2014; 7:417–427. [PubMed: 24022789]
42. Jin J-O, Yu QT. Cell-Associated Cytokines in the Pathogenesis of Sjögren's Syndrome. J Clin Cell Immunol. 2013; S!:11742. [PubMed: 23814683]

43. Wang B, Andre I, Gonzalez A, Katz JD, Aguet M, Benoist C, et al. Interferon-gamma impacts at multiple points during the progression of autoimmune diabetes. Proc Natl Acad Sci U S A. 1997; 94:13844–13849. [PubMed: 9391115]
44. Nicoletti F, Zaccone P, Di Marco R, Di Mauro M, Magro G, Grasso S, et al. The effects of a nonimmunogenic form of murine soluble interferon-gamma receptor on the development of autoimmune diabetes in the NOD mouse. Endocrinology. 1996; 137:5567–5575. [PubMed: 8940385]
45. Peng SL, Moslehi J, Craft J. Roles of interferon-gamma and interleukin-4 in murine lupus. J Clin Invest. 1997; 99:1936–1946. [PubMed: 9109438]
46. Theofilopoulos AN, Koundouris S, Kono DH, Lawson BR. The role of IFN-gamma in systemic lupus erythematosus: a challenge to the Th1/Th2 paradigm in autoimmunity. Arthritis Res. 2001; 3:136–141. [PubMed: 11299053]
47. Boissier MC, Chiocchia G, Bessis N, Hajnal J, Garotta G, Nicoletti F, et al. Biphasic effect of interferon-gamma in murine collagen-induced arthritis. Eur J Immunol. 1995; 25:1184–1190. [PubMed: 7774621]
48. Fox RI, Kang HI, Ando D, Abrams J, Pisa E. Cytokine mRNA expression in salivary gland biopsies of Sjogren's syndrome. J Immunol. 1994; 152:5532–5539. [PubMed: 8189070]
49. Boumba D, Skopouli FN, Moutsopoulos HM. Cytokine mRNA expression in the labial salivary gland tissues from patients with primary Sjogren's syndrome. Br J Rheumatol. 1995; 34:326–333. [PubMed: 7788146]
50. Cha S, Brayer J, Gao J, Brown V, Killedar S, Yasunari U, et al. A dual role for interferon-gamma in the pathogenesis of Sjogren's syndrome-like autoimmune exocrinopathy in the nonobese diabetic mouse. Scand J Immunol. 2004; 60:552–565. [PubMed: 15584966]
51. Baker OJ, Camden JM, Redman RS, Jones JE, Seye CI, Erb L, et al. Proinflammatory cytokines tumor necrosis factor-alpha and interferon-gamma alter tight junction structure and function in the rat parotid gland Par-C10 cell line. Am J Physiol Cell Physiol. 2008; 295:C1191–1201. [PubMed: 18768927]
52. Matsumura R, Umemiya K, Goto T, Nakazawa T, Ochiai K, Kagami M, et al. Interferon gamma and tumor necrosis factor alpha induce Fas expression and anti-Fas mediated apoptosis in a salivary ductal cell line. Clin Exp Rheumatol. 2000; 18:311–318. [PubMed: 10895367]
53. Ogawa N, Ping L, Zhenjun L, Takada Y, Sugai S. Involvement of the interferon-gamma-induced T cell-attracting chemokines, interferon-gamma-inducible 10-kd protein (CXCL10) and monokine induced by interferon-gamma (CXCL9), in the salivary gland lesions of patients with Sjogren's syndrome. Arthritis Rheum. 2002; 46:2730–2741. [PubMed: 12384933]
54. Yoon KC, Park CS, You IC, Choi HJ, Lee KH, Im SK, et al. Expression of CXCL9, -10, -11, and CXCR3 in the tear film and ocular surface of patients with dry eye syndrome. Invest Ophthalmol Vis Sci. 2010; 51:643–650. [PubMed: 19850844]
55. Kamao T, Miyazaki T, Soga Y, Komori H, Terada M, Ohashi Y, et al. Genetic dissociation of dacryoadenitis and sialadenitis in a Sjogren's syndrome mouse model with common and different susceptibility gene loci. Invest Ophthalmol Vis Sci. 2009; 50:3257–3265. [PubMed: 19218603]
56. Bettelli E, Carrier Y, Gao W, Korn T, Strom TB, Oukka M, et al. Reciprocal developmental pathways for the generation of pathogenic effector TH17 and regulatory T cells. Nature. 2006; 441:235–238. [PubMed: 16648838]
57. Skarstein K, Wahren M, Zaura E, Hattori M, Jonsson R. Characterization of T cell receptor repertoire and anti-Ro/SSA autoantibodies in relation to sialadenitis of NOD mice. Autoimmunity. 1995; 22:9–16. [PubMed: 8882417]
58. Schneider CA, Rasband WS, Eliceiri KW. NIH Image to ImageJ: 25 years of image analysis. Nat Methods. 2012; 9:671–675. [PubMed: 22930834]
59. Lamoreaux L, Roederer M, Koup R. Intracellular cytokine optimization and standard operating procedure. Nat Protoc. 2006; 1:1507–1516. [PubMed: 17406442]
60. Van den Broeck W, Derore A, Simoens P. Anatomy and nomenclature of murine lymph nodes: Descriptive study and nomenclatory standardization in BALB/cAnNCrl mice. J Immunol Methods. 2006; 312:12–19. [PubMed: 16624319]

61. Duan WR, Garner DS, Williams SD, Funckes-Shippy CL, Spath IS, Blomme EA. Comparison of immunohistochemistry for activated caspase-3 and cleaved cytokeratin 18 with the TUNEL method for quantification of apoptosis in histological sections of PC-3 subcutaneous xenografts. J Pathol. 2003; 199:221–228. [PubMed: 12533835]

62. Price LC, Shao D, Meng C, Perros F, Garfield BE, Zhu J, et al. Dexamethasone induces apoptosis in pulmonary arterial smooth muscle cells. Respir Res. 2015; 16:114. [PubMed: 26382031]

63. Finkin S, Yuan D, Stein I, Taniguchi K, Weber A, Unger K, et al. Ectopic lymphoid structures function as microniches for tumor progenitor cells in hepatocellular carcinoma. Nat Immunol. 2015; 16:1235–1244. [PubMed: 26502405]

64. Chen YC, Kuo HY, Bornschein U, Takahashi H, Chen SY, Lu KM, et al. Foxp2 controls synaptic wiring of corticostriatal circuits and vocal communication by opposing Mef2c. Nat Neurosci. 2016; 19:1513–1522. [PubMed: 27595386]

65. Dai Y, Jia P, Fang Y, Liu H, Jiao X, He JC, et al. miR-146a is essential for lipopolysaccharide (LPS)-induced cross-tolerance against kidney ischemia/reperfusion injury in mice. Sci Rep. 2016; 6:27091. [PubMed: 27250735]

66. Hunninghake GW, Doerschug KC, Nymon AB, Schmidt GA, Meyerholz DK, Ashare A. Insulin-like growth factor-1 levels contribute to the development of bacterial translocation in sepsis. Am J Respir Crit Care Med. 2010; 182:517–525. [PubMed: 20413631]

67. Gibson-Corley KN, Olivier AK, Meyerholz DK. Principles for valid histopathologic scoring in research. Vet Pathol. 2013; 50:1007–1015. [PubMed: 23558974]

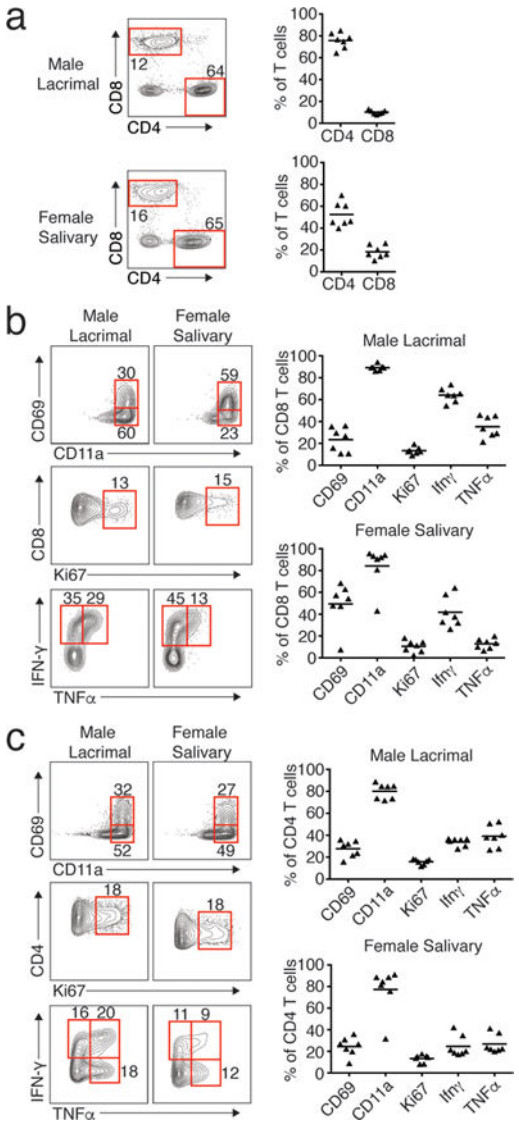

Figure 1. Gland-infiltrating CD8 T cells display an activated phenotype

(a) Representative flow cytometry plots of gland-infiltrating T cells from male lacrimal (top) or female salivary (bottom) glands from 12–17 week-old NOD mice. Plots were gated on live, CD3ε$^+$ singlets. Numbers represent the frequency of cells in indicated gate. Graphs depict cumulative quantification of data from at least 2 independent experiments from male lacrimal (top) or female salivary (bottom) glands, $n = 7$ per group. Each data point indicates an individual mouse and lines represent the mean. **(b)** Flow cytometric analyses of gland-infiltrating CD8 T cells from male lacrimal (left) or female salivary (right) glands from mice in a. Plots were gated on live, CD3ε$^+$CD8$^+$CD4$^-$ singlets. Numbers represent the frequency of cells in each gate. **(c)** Flow cytometric analyses of gland-infiltrating CD4 T cells from male lacrimal (left) or female salivary (right) glands from mice in a. Plots were gated on live, CD3ε$^+$CD8$^-$CD4$^+$Foxp3$^-$ singlets. Numbers represent the frequency of cells in each gate.

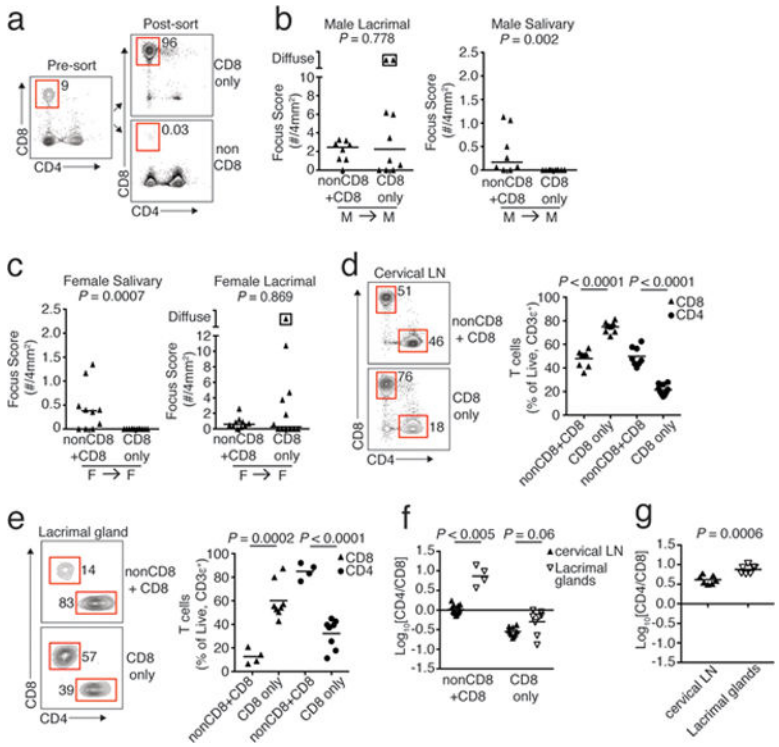

Figure 2. Transfer of CD8 T cells causes dacryoadenitis, but not sialadenitis, in NOD-SCID recipients

(a) Representative plots to demonstrate CD8 T cells in pre- and post-sort samples. Bulk cervical LN cells from male NOD mice were FACSorted into purified CD8 cells (CD8 only) or CD8-depleted cells (nonCD8). Plots were gated on singlets. Numbers represent the frequency of cells in indicated gate. **(b)** Quantification of lacrimal (left) and salivary (right) gland inflammation in male NOD-SCID recipients of male NOD donor cells. Recipients received CD8-depleted cells with CD8 T cells added back (nonCD8+CD8: $n = 8$) or purified CD8 T cells alone (CD8 only: $n = 10$). Data are pooled from at least 2 independent experiments. Symbols represent individual mice, lines are medians. Boxed symbols represent diffuse inflammation in which individual foci coalesced and could not be accurately enumerated. *P* values determined by Mann-Whitney *U*-test. **(c)** Quantification of salivary (left) and lacrimal (right) gland inflammation in female NOD-SCID recipients of female NOD donor cells. Recipients received nonCD8+CD8: $n = 10$ or CD8 only: $n = 12$. Data are pooled from 2 independent experiments. Symbols represent individual mice, lines are medians. *P* value determined by Mann-Whitney *U*-test. **(d and e)** Representative flow cytometry plots of cervical LN cells (d) or lacrimal gland-infiltrating cells (e) from male recipients represented in b. Plots were gated on live, CD3ε$^+$ singlets. Numbers represent the frequency of cells in indicated gate. Graphs depict cumulative quantification of data pooled from 2 independent experiments (nonCD8+CD8: $n = 8$; CD8 only: $n = 10$) (d) or 1 experiment (nonCD8+CD8: $n = 4$; CD8 only: $n = 8$) (e). Each symbol represents an individual mouse, lines are means. *P* values determined by unpaired Student's *t*-test. **(f)** Ratio of CD4 to CD8 T cells (log transformed) present in the cervical LN or lacrimal glands of male recipients from d and e. Each symbol represents an individual mouse, lines are means. *P* values determined by unpaired Student's *t*-test. **(g)** Ratio of CD4 to CD8 T cells

(log transformed) present in spontaneous male NOD mouse lacrimal gland infiltrates. Data are representative of 2 independent experiments ($n = 7$). Each symbol represents an individual mouse, lines are means. P value determined by unpaired Student's t-test.

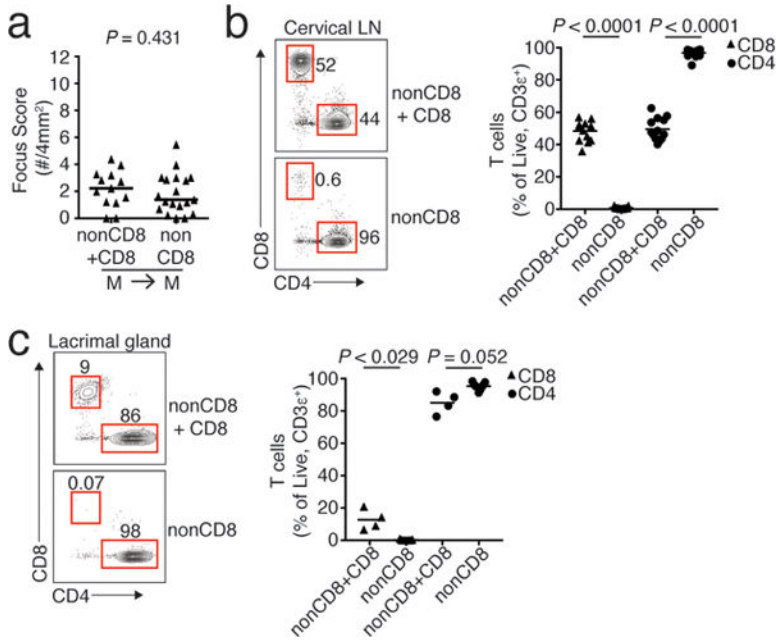

Figure 3. Lacrimal gland inflammation occurs in the absence of CD8 T cells

(a) Quantification of lacrimal gland inflammation in male NOD-SCID recipients of sorted male NOD donor cervical LN cells. Recipients received CD8-depleted cells with CD8 T cells added back (nonCD8+CD8; $n = 13$) or CD8-depleted cells alone (nonCD8; $n = 19$). Data are pooled from 3 independent experiments. Symbols represent individual mice, lines are medians. *P* value determined by Mann-Whitney *U*-test. **(b)** Representative flow cytometry plots of cells isolated from the cervical LN from recipients in a. Plots were gated on live, CD3ε$^+$ singlets. Numbers represent the frequency of cells in indicated gates. Graphs depict cumulative quantification of data pooled from 3 independent experiments. Symbols represent individual recipients, lines are means. *P* values determined by unpaired Student's *t*-test. **(c)** Representative flow cytometry plots of cells isolated from the lacrimal glands from recipients in a. Plots were gated on live, CD3ε$^+$ singlets. Numbers represent the frequency of cells in indicated gates. Graphs depict cumulative quantification of data from 1 experiment (nonCD8+CD8: $n = 4$; 8 only: $n = 9$). Symbols represent individual recipients, lines are means. *P* values determined by unpaired Student's *t*-test.

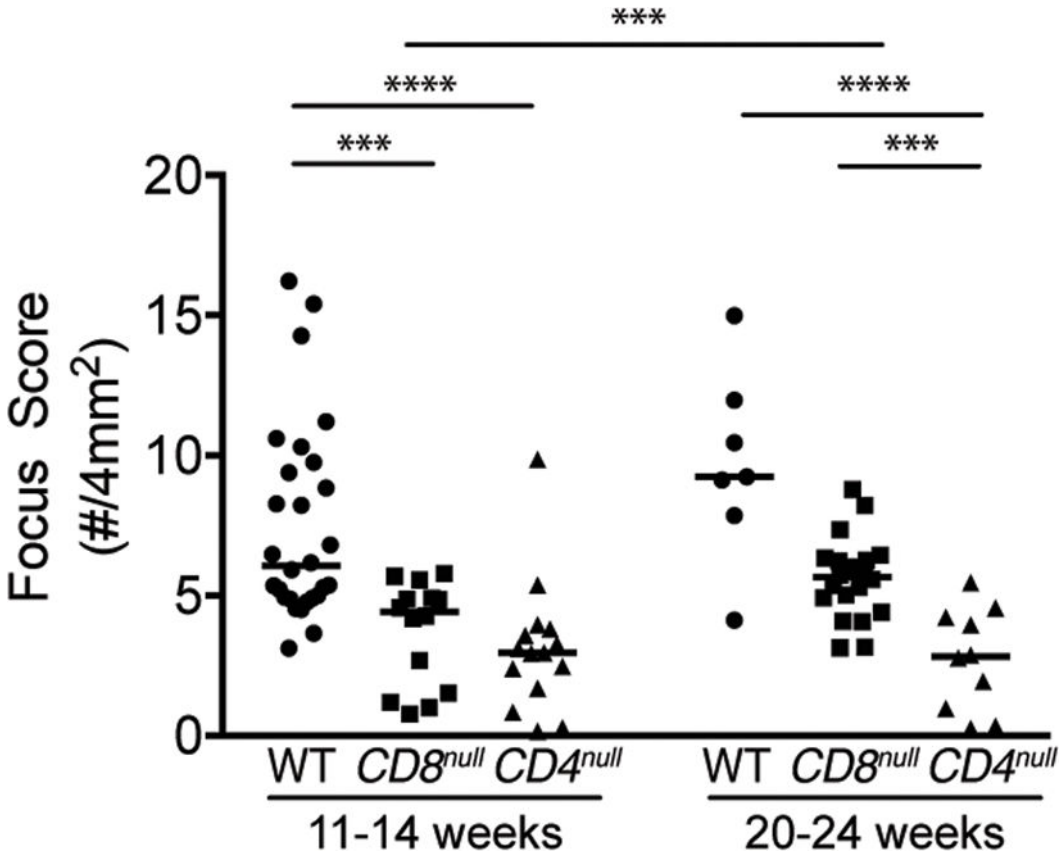

Figure 4. CD8 and CD4 T cells each contribute to the early stages of lacrimal gland autoimmunity

Quantification of inflammation in male lacrimal glands from 11–14 week old WT ($n = 28$), $CD8^{null}$ ($n = 14$), or $CD4^{null}$ ($n = 15$) NOD mice or 20–24 week old WT ($n = 7$), $CD8^{null}$ ($n = 20$), or $CD4^{null}$ ($n = 10$) NOD mice. Symbols represent individual mice, lines represent medians. Significant differences between mouse groups and age groups were identified by two-way ANOVA on focus score ranks ($P < 0.0001$ and $P < 0.01$, respectively) with no significant interaction between the two ($P = 0.109$). Tukey's HSD post-hoc test P values are shown. * $P < 0.05$, *** $P < 0.001$, **** $P < 0.0001$.

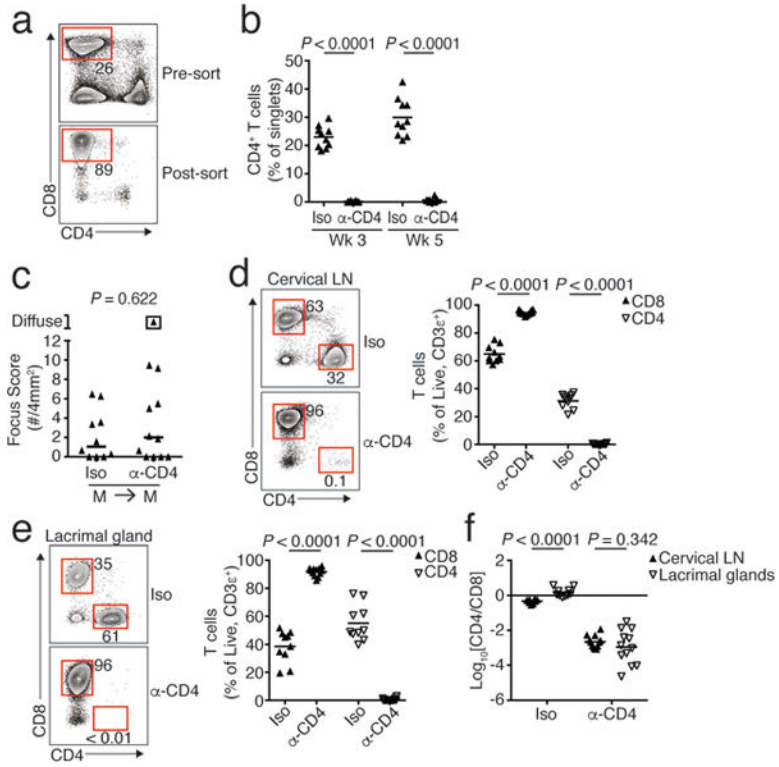

Figure 5. CD8 T cells cause dacryoadenitis in the absence of CD4 T cells

(a) Representative flow cytometry plots to demonstrate CD8 T cells in pre- and post-sort samples. Bulk cervical LN cells from male NOD mice were FACSorted based on expression of CD8α. Plots were gated on singlets. Numbers represent the frequency of cells in indicated gate. **(b)** Cumulative quantification of CD4 T cells in the peripheral blood of male NOD-SCID recipient mice that received purified CD8 T cells from male NOD donors and were treated weekly with anti-CD4 antibody ($n = 12$) or isotype control antibody ($n = 10$). Data are representative of 2 independent experiments. Symbols represent individual mice, lines represent means. *P* values determined by unpaired Student's *t*-test. **(c)** Quantification of lacrimal gland inflammation in male NOD-SCID recipients in b. Symbols represent individual mice, lines represent medians. *P* value determined by Mann-Whitney *U*-test. **(d and e)** Representative flow cytometry plots of cells isolated from the cervical LN (d) or lacrimal glands (e) of male NOD-SCID recipient mice treated as in b. Plots were gated on live, $CD3\varepsilon^+$ singlets. Graphs depict cumulative quantification of CD8 or CD4 T cells pooled from 2 independent experiments. Symbols represent individual mice, lines represent means. *P* values determined by unpaired Student's *t*-test. **(f)** Ratio of CD4 to CD8 T cells (log transformed) present in the cervical LN or lacrimal glands of male recipients from b. Each symbol represents an individual mouse, lines are means. Data are representative of 2 independent experiments. *P* values determined by unpaired Student's *t*-test.

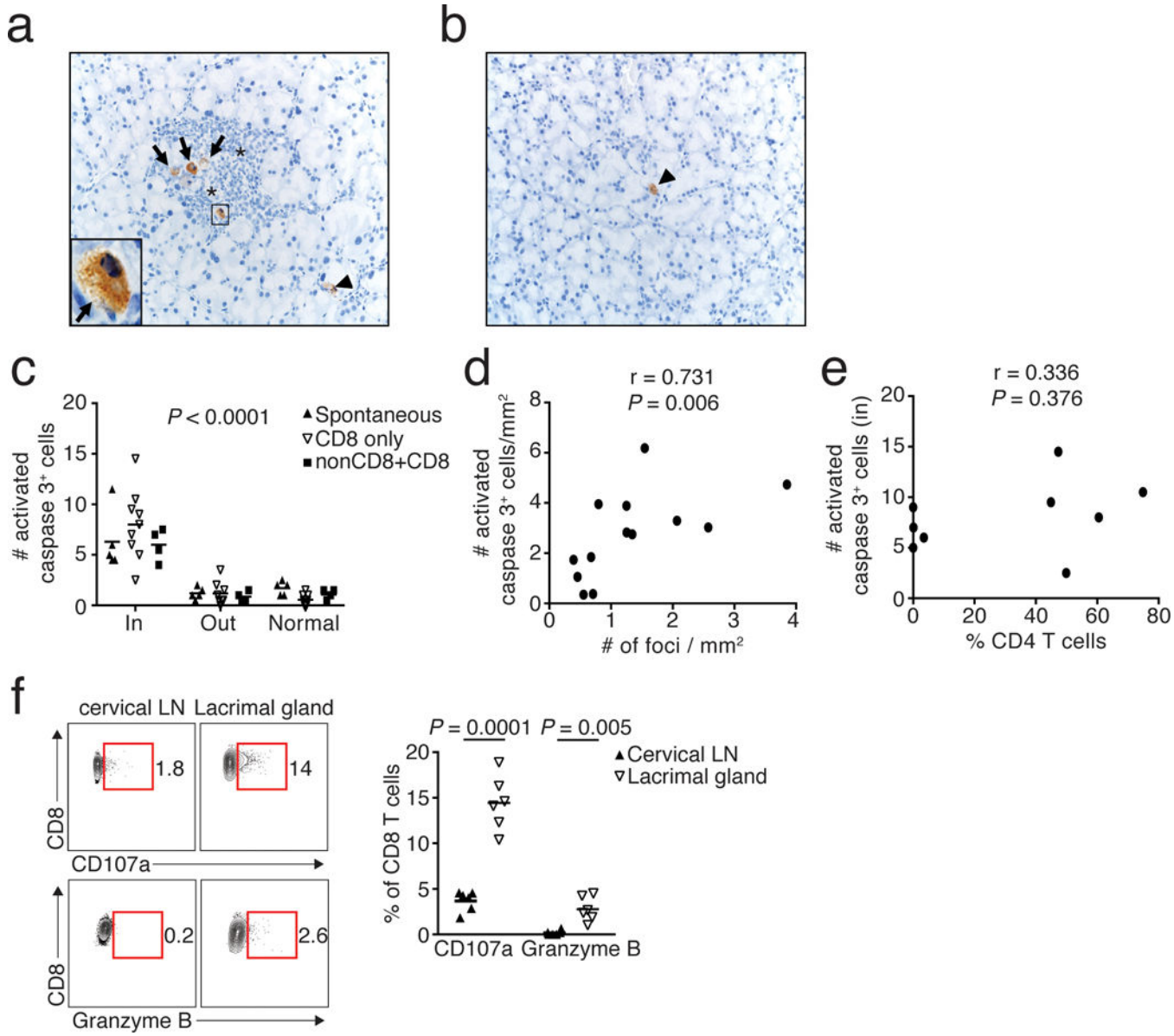

Figure 6. CD8 T cells mediate destruction of lacrimal gland epithelial cells

(a and b) Activated caspase-3 immunostaining. Representative microscopic fields of lacrimal glands with focus of inflammation (a, asterisks) or lacking inflammation (b). Arrows and inset represent activated caspase-3$^+$ cells located within the inflammatory focus (a). Arrowheads represent activated caspase-3$^+$ cells located outside of inflammatory cell focus (a) or in area of normal tissue devoid of inflammatory foci (b). **(c)** Quantification of the number of activated caspase-3$^+$ cells in lacrimal gland sections from NOD mice that spontaneously developed lacrimal gland inflammation ($n = 5$), or NOD-SCID mice that received CD8 only cells ($n = 9$) or nonCD8+CD8 cells ($n = 4$) based on location: within inflammatory foci (in), outside of inflammatory foci (out), or in areas of normal gland tissue (normal). Activated caspase-3$^+$ cells were determined by averaging the values from 2 images per gland. Symbols represent individual mice, lines are means. *P* value determined by two-

way ANOVA demonstrates a significant difference between locations (i.e., for each group "in" is greater than "out" or "normal") but no significant difference between groups (P = 0.68) and no significant interaction between group and location (P = 0.34). **(d)** Correlation between the total number of activated caspase-3^+ cells per mm^2 and the number of foci per mm^2 in whole lacrimal gland sections from recipients of CD8 only cells (n = 4), recipients of nonCD8+CD8 cells (n = 4), or male NOD mice with spontaneous disease (n = 5). Symbols represent individual mice. P and r values were determined by Spearman correlation. **(e)** Correlation between the number of activated caspase-3^+ cells within foci and percentage of CD4 T cells in the lacrimal glands of mice that received CD8 only T cells. Symbols represent individual mice. P and r values were determined by Pearson correlation. **(f)** Flow cytometric analyses of CD8 T cells isolated from the cervical LN or lacrimal glands of 12–16-week old male NOD mice. Cells were gated on live, $CD3\varepsilon^+CD19^-CD8^+$ singlets prior to assessing surface expression of CD107a or staining for intracellular granzyme B. Numbers represent the frequency of cells in each gate. Graphs depict cumulative quantification of data from 2 independent experiments (n = 6 per group). P values determined by unpaired Student's t-test.